Supplementary Information

Thermally activated delayed fluorescence emitters with a *m,m*-di-*tert*-butyl-carbazolyl benzoylpyridine core achieving extremely high blue electroluminescence efficiencies

Pachaiyappan Rajamalli,[a] Vasudevan Thangaraji,[a] Natarajan Senthilkumar,[a] Chen-Cheng Ren-Wu,[b] Hao-Wu Lin[b] and Chien-Hong Cheng*[,a]

[a]Department of Chemistry, National Tsing Hua University,
Hsinchu 30013, Taiwan
E-mail: chcheng@mx.nthu.edu.tw

[b]Department of Materials Science and Engineering, National Tsing Hua University,
Hsinchu 30013, Taiwan.

General Information

The ^{1}H and ^{13}C NMR spectra were recorded by using Varian mercury 400 spectrometer. The HRMS were measured using MAT-95XL HRMS or MStation. The UV-visible absorption spectra were taken on a Hitachi U-3300 spectrophotometer. Fluorescence and phosphorescence spectra were recorded on a Hitachi F-7000 spectrophotometer. The decomposition temperature was determined by TGA using TG/DTA Seiko SSC-5200 instrument. Transient PL measurement of the materials in solution were obtained using 355 nm pulsed laser (Nd:YAG laser, INDI-40-10, Spectra-Physics) as the excitation source and the sample was excited by the optical fiber (77532, Newport Corp). A highpass filter (GG-400-25.4, Lamda) at 410 nm in front of the photodiode (DET10A/M, Thorlabs) was used to prevent the scattering of 355-nm laser. The electronic signal was recorded by an oscilloscope (WaveSurfer 24MXs-B, LeCroy). The absolute PL quantum efficiency of the doped films were determined using an integrating sphere under N_2 atmosphere. The electrochemical properties were measured by using CH Instruments 600A electrochemical analyzer. The oxidation measurements were measured using a glassy carbon electrode as the

working electrode, an Ag/Ag^+ (0.01 M $AgNO_3$) as the reference electrode and a Pt wire as the counter electrode in dichloromethane. The HOMO energy level were determined from the onset of the oxidation potential using the equation -(4.8 eV + E_{ox} (vs Fc_{ox})).

DFT Calculation

Molecular geometry optimizations and electronic properties were carried out by using the Gaussian 03 program with density functional theory (DFT) and time-dependent DFT (TDDFT) calculations in which the Becke's three parameter functional combined with Lee, Yang, and Parr's correlation functional (B3LYP) hybrid exchange-correlation functional with the 6-31G* basic set were used.[1] The molecular orbitals were visualized using Gaussview 4.1 software.

OLEDs Fabrication and Measurement

The organic materials used in device fabrication were purified by sublimation. Devices were fabricated by vacuum deposition onto pre-coated ITO glass with sheet resistance of 15 Ω/square at a pressure lower than 10^{-6} Torr. The organic materials were deposited at the rate of 0.5~1.2 Å s^{-1}. LiF and Al were deposited at the rate of 0.1 Å s^{-1}, 3-10 Å s^{-1}, respectively. The rest of the procedures are similar to the reported method.[2]

The transient EL measurements were carried out on a function generator (Agilent 8114A) and an indigenously developed time-resolved emission spectrometer. The devices were driven by a voltage pulse 6 V with a repetition rate of 20 kHz and pulse width of 10 μs. The emission decay curves at specific wavelengths were gained using a cooled photomultiplier tube (PMT) detector (Becker & Hickl GmbH PMC-100) integrated with a 300 nm focal length monochromator (Princeton Instruments Acton SP2300). The time-resolved photon counting was done via a multi-channel scaling (MCS) card (Becker & Hickl GmbH MSA-300) with a time resolution of 5 ns.

The whole system was synchronized with a digital delay generator (Stanford Research Systems DG645).

Table S1. Main transitions and electron contour plots of molecular orbitals of 4BPy-*m*DTC

Transition	Orbitals	Probabilities	f^a
$S_0 \rightarrow S_1$	HOMO→LUMO HOMO-1→LUMO	0.67741 0.18881	0.0185
$S_0 \rightarrow S_2$	HOMO→LUMO HOMO-1→LUMO	0.19037 0.67830	0.0079
$S_0 \rightarrow S_6$	HOMO→LUMO+1 HOMO→LUMO+2 HOMO-1→LUMO+1 HOMO-1→LUMO+2	0.49121 0.30790 0.29808 0.24116	0.2187

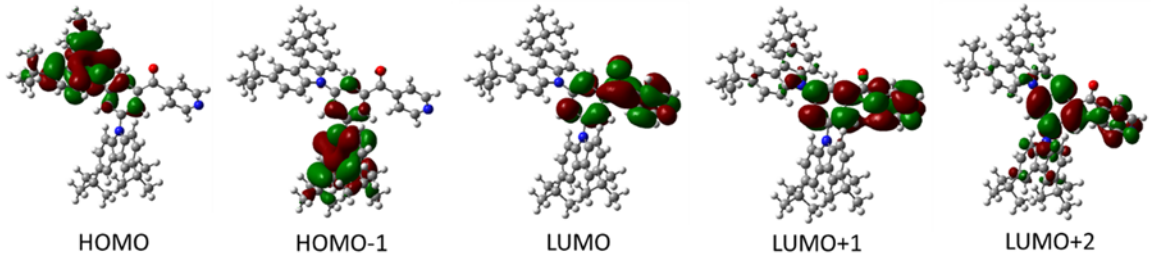

Table S2. Main transitions and electron contour plots of molecular orbitals of 3BPy-*m*DTC

Transition	Orbitals	Probabilities	f^a
$S_0 \rightarrow S_1$	HOMO→LUMO HOMO-1→LUMO	0.66142 0.23662	0.0231
$S_0 \rightarrow S_2$	HOMO→LUMO HOMO-1→LUMO	0.23857 0.66268	0.0056
$S_0 \rightarrow S_6$	HOMO→LUMO+1 HOMO→LUMO+2 HOMO→LUMO+4 HOMO-1→LUMO+1 HOMO-1→LUMO+2 HOMO-1→LUMO+4	0.36942 0.27188 0.20215 0.37119 0.24757 0.19548	0.2152

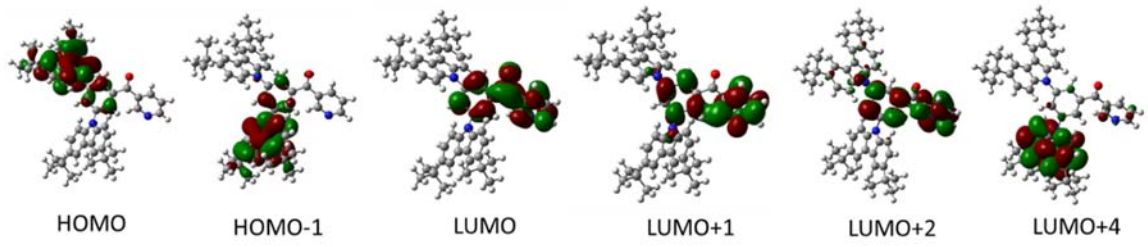

Table S3. Main transitions and electron contour plots of molecular orbitals of 2BPy-*m*DTC

Transition	Orbitals	Probabilities	f^a
$S_0 \rightarrow S_1$	HOMO→LUMO HOMO-1→LUMO	0.67045 0.21482	0.0105
$S_0 \rightarrow S_2$	HOMO→LUMO HOMO-1→LUMO	0.21511 0.67151	0.0043
$S_0 \rightarrow S_6$	HOMO→LUMO+1 HOMO→LUMO+2 HOMO-1→LUMO+1	0.50359 0.10802 0.46807	0.0284

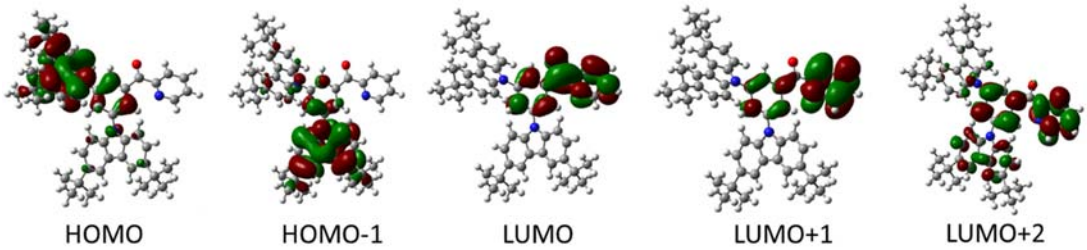

Table S4. Main transitions and electron contour plots of molecular orbitals of BP-*m*DTC

Transition	Orbitals	Probabilities	f^a
$S_0 \rightarrow S_1$	HOMO→LUMO HOMO-1→LUMO	0.68062 0.17147	0.0250
$S_0 \rightarrow S_2$	HOMO→LUMO HOMO-1→LUMO	0.17480 0.68138	0.0093
$S_0 \rightarrow S_6$	HOMO→LUMO+1 HOMO-1→LUMO+1	0.55396 0.40185	0.2362

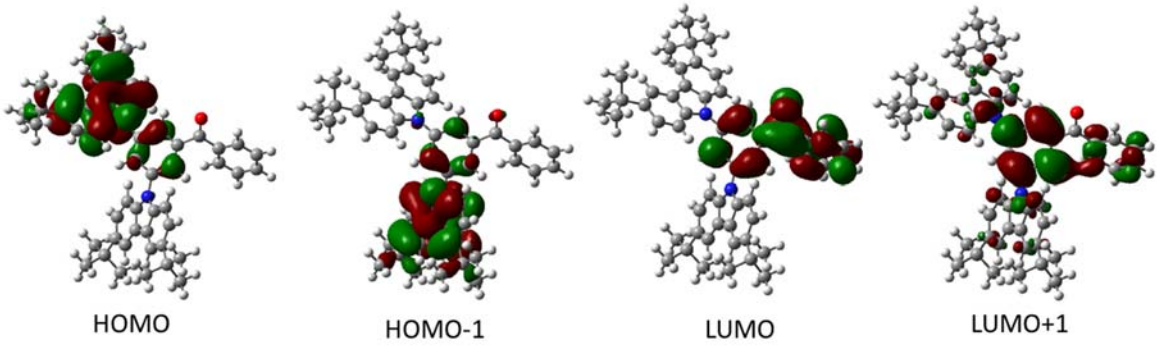

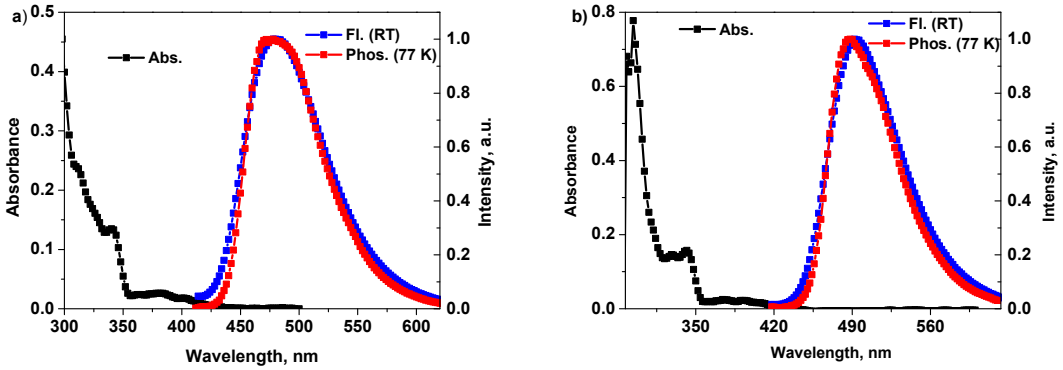

Fig. S1 Absorption (Abs.) and fluorescence (Fl.) spectra of 3BPy-*m*DTC (a) and 2BPy-*m*DTC (b) in toluene (10^{-5} M) solution measured at room temperature and phosphorescence (Phos.) spectra in toluene (10^{-5} M) measured at 77 K.

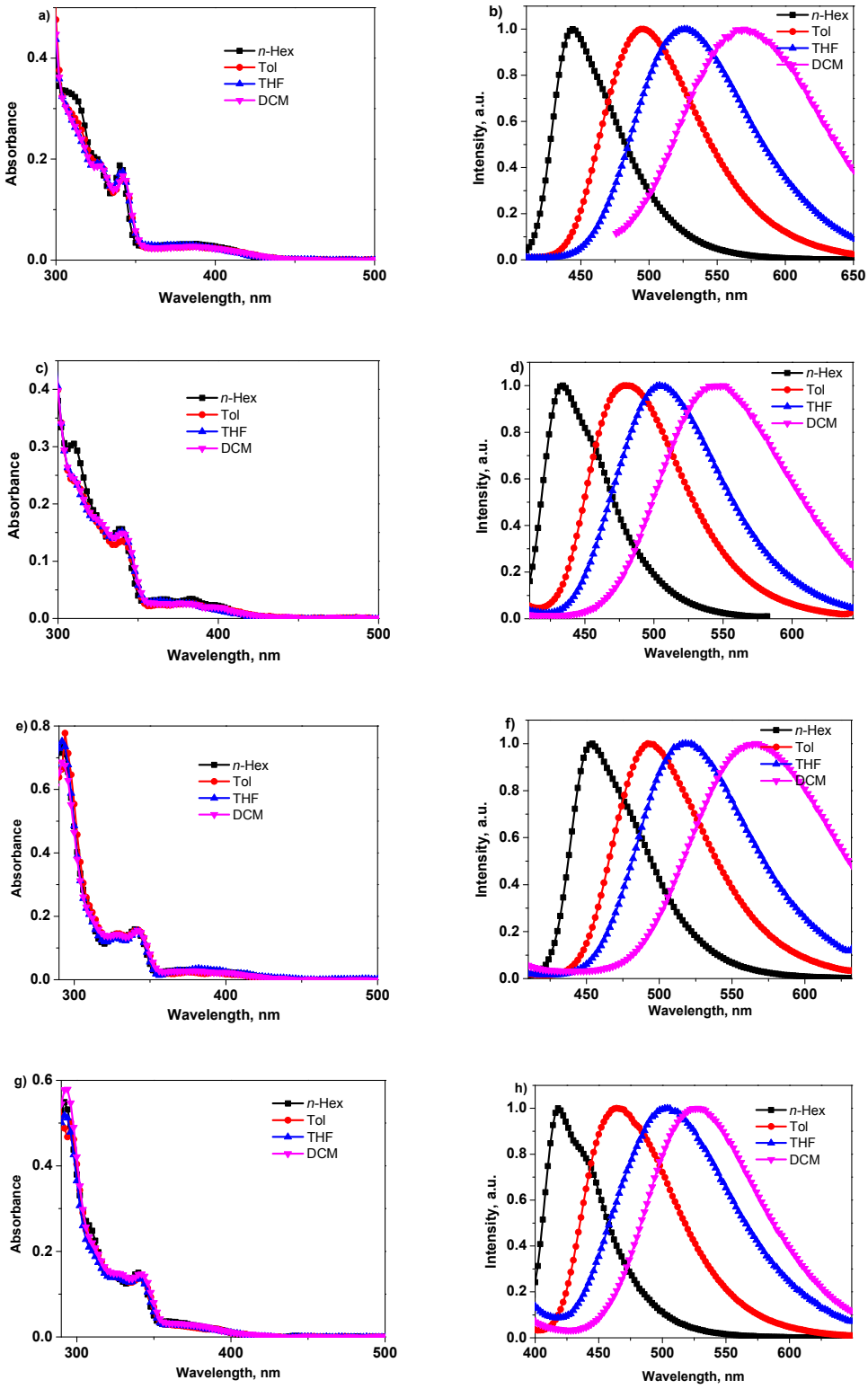

Fig. S2 Absorbance spectra and fluorescence spectra of 4BPy-*m*DTC (a and b), 3BPy-*m*DTC (c and d) 2BPy-*m*DTC (e and f) and BP-*m*DTC (g and h) in various solvents at RT (10^{-5} M).

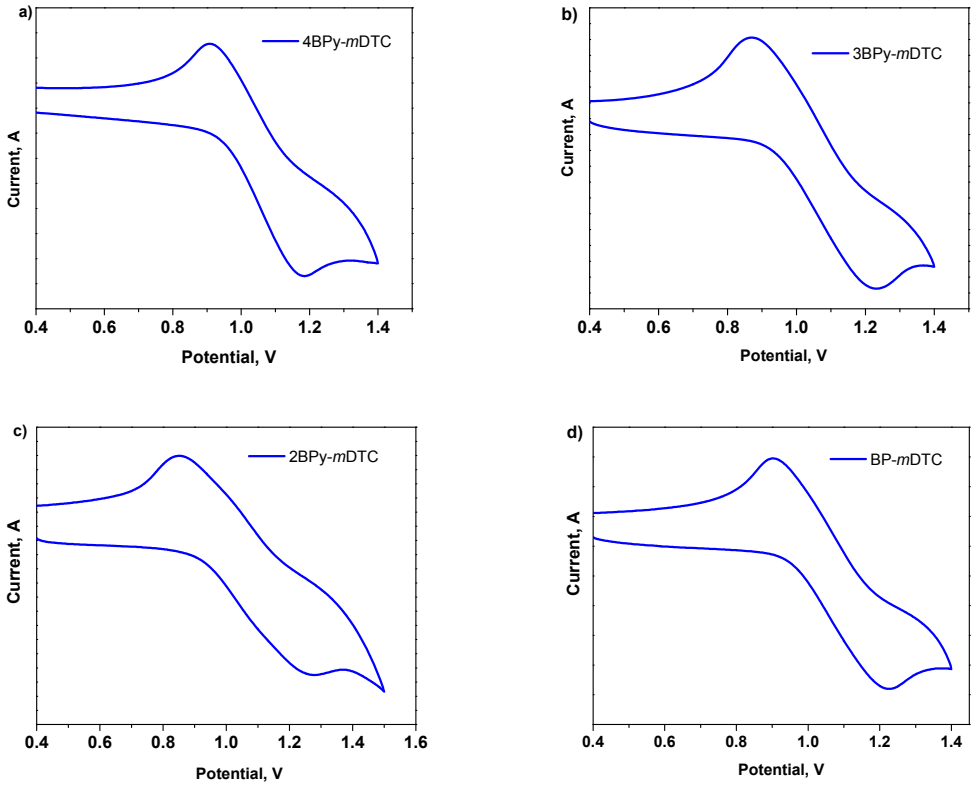

Fig. S3 Oxidization potentials of a) 4BPy-*m*DTC, b) 3BPy-*m*DTC, c) 2BPy-*m*DTC and d) BP-*m*DTC and were measured in 10^{-3} M DCM. The electrode potentials were measured versus Ag/Ag^{+} electrode.

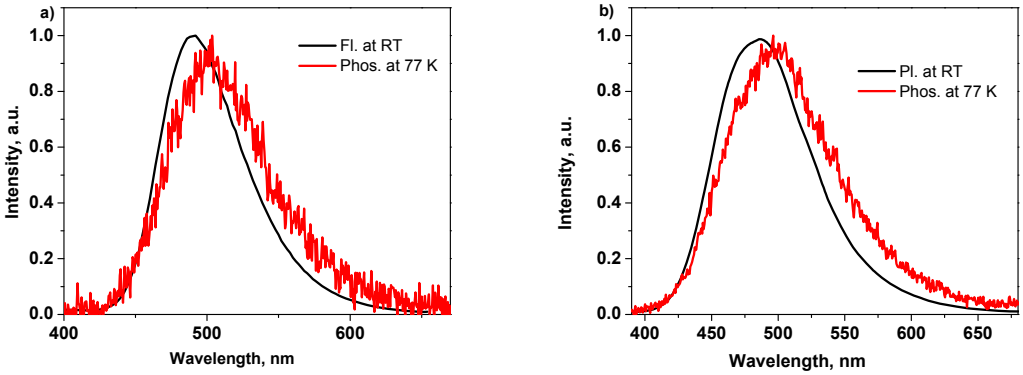

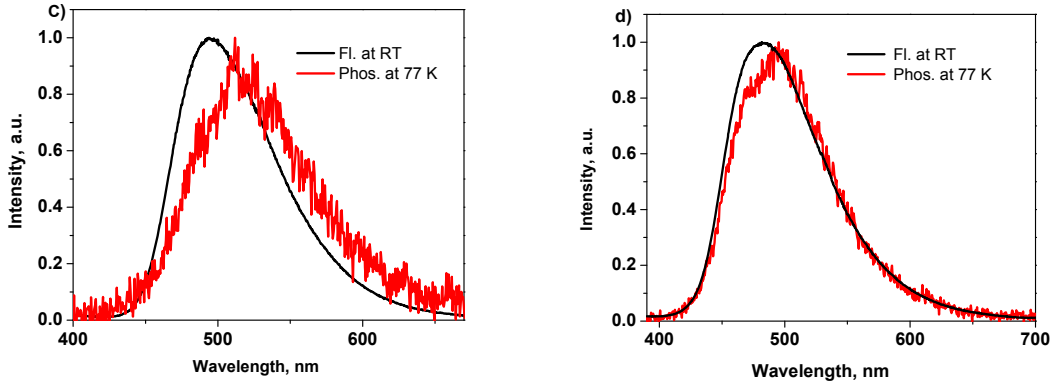

Fig. S4 Fluorescence (Fl.) and phosphorescence (Phos.) spectra of 7 wt% a) 4BPy-*m*DTC, b) 3BPy-*m*DTC, c) 2BPy-*m*DTC and d) BP-*m*DTC doped in *m*CBP films. Fluorescence spectra were measured at room temperature and phosphorescence spectra were measured at 77 K.

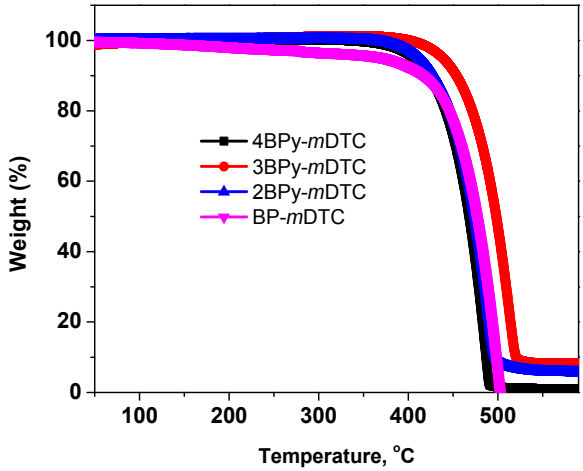

Fig. S5 The thermogravimetric thermograms of 4BPy-*m*DTC, 3BPy-*m*DTC, 2BPy-*m*DTC and BP-*m*DTC.

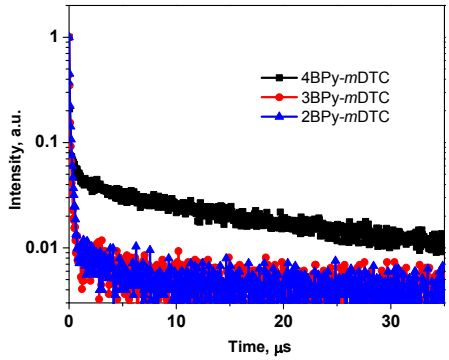

Fig. S6 Transient PL characteristics of co-doped films (7 wt% 4BPy-*m*DTC, 3BPy-*m*DTC, or 2BPy-*m*DTC doped in *m*CBP host) at 300 K.

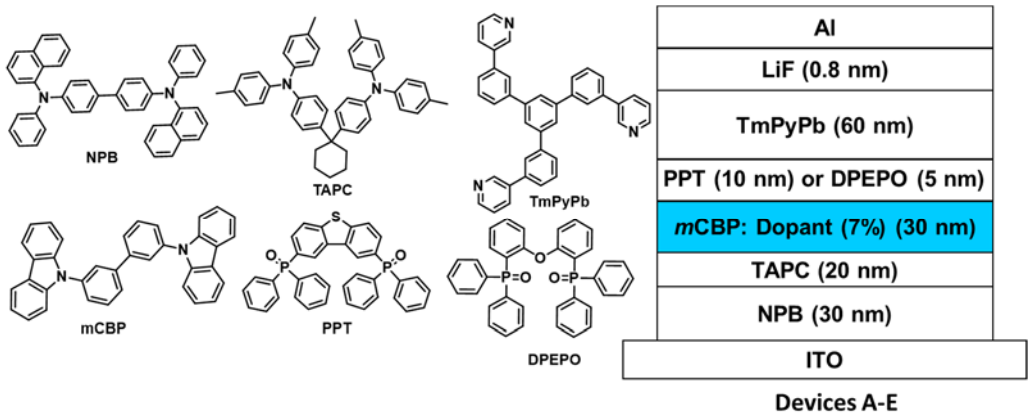

Fig. S7 Structures of the materials used in devices and schematic representation of devices A-E.

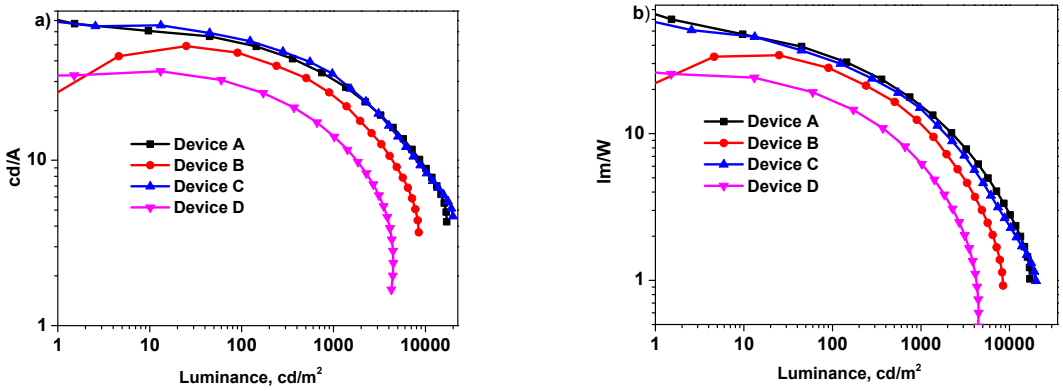

Fig. S8 a) The current efficiency vs luminance, b) power efficiency vs luminance of devices A-D.

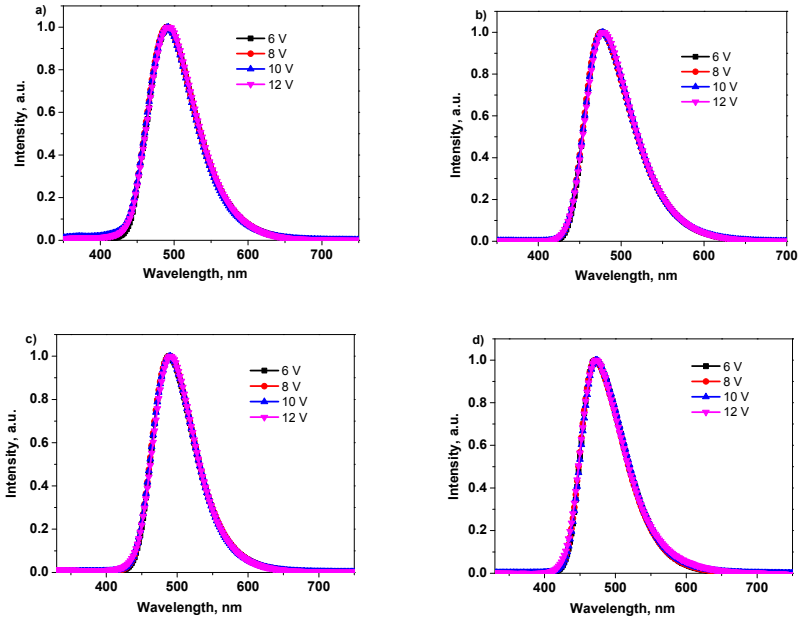

Fig. S9 El spectra at various voltages of a) device A, b) device B, c) device C, and d) device D.

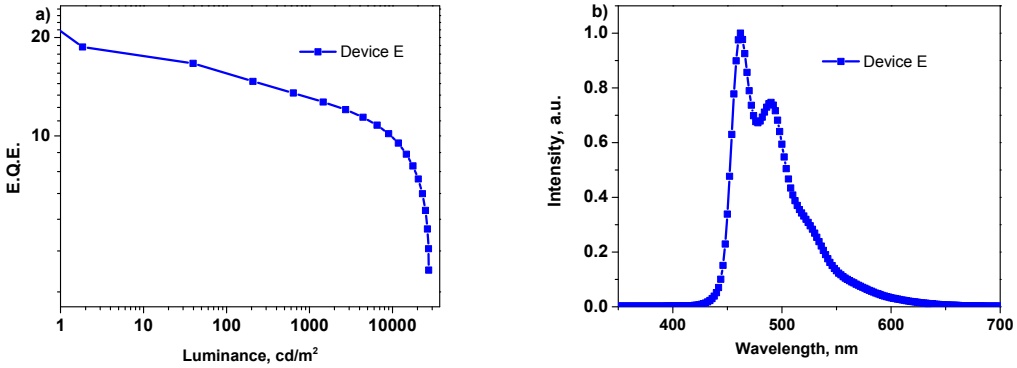

Fig. S10 a) EQE vs luminance and b) electroluminescence spectra of device E.

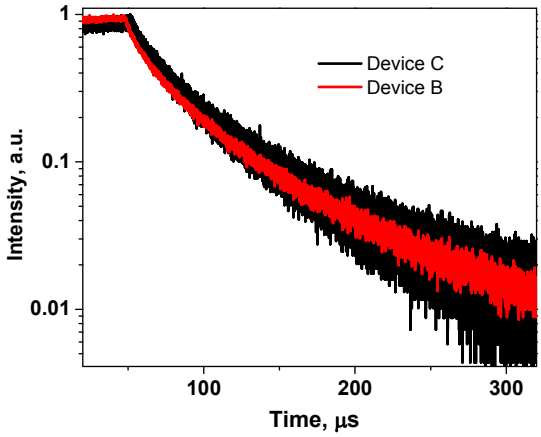

Fig. S11 Transient electroluminescence characteristics of devices B and C.

a)

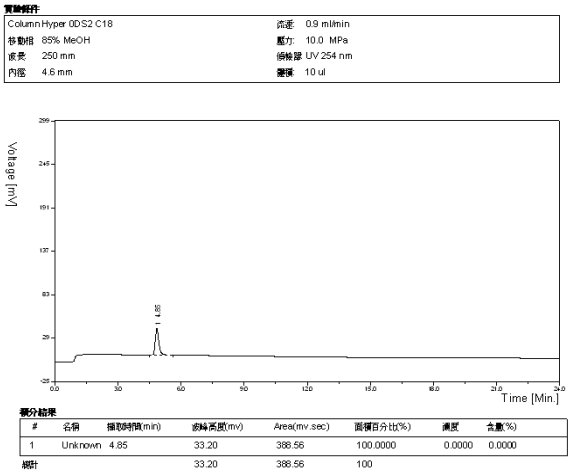

b)

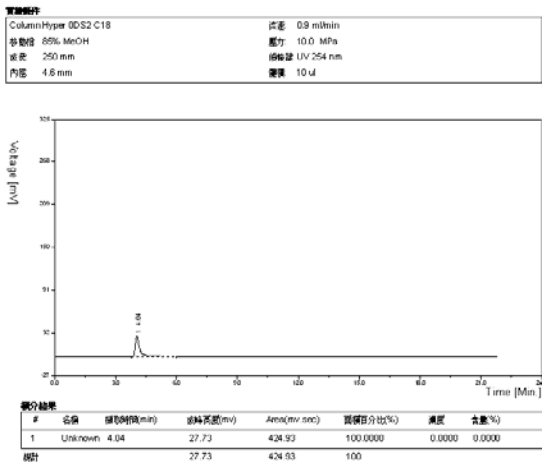

c) d)

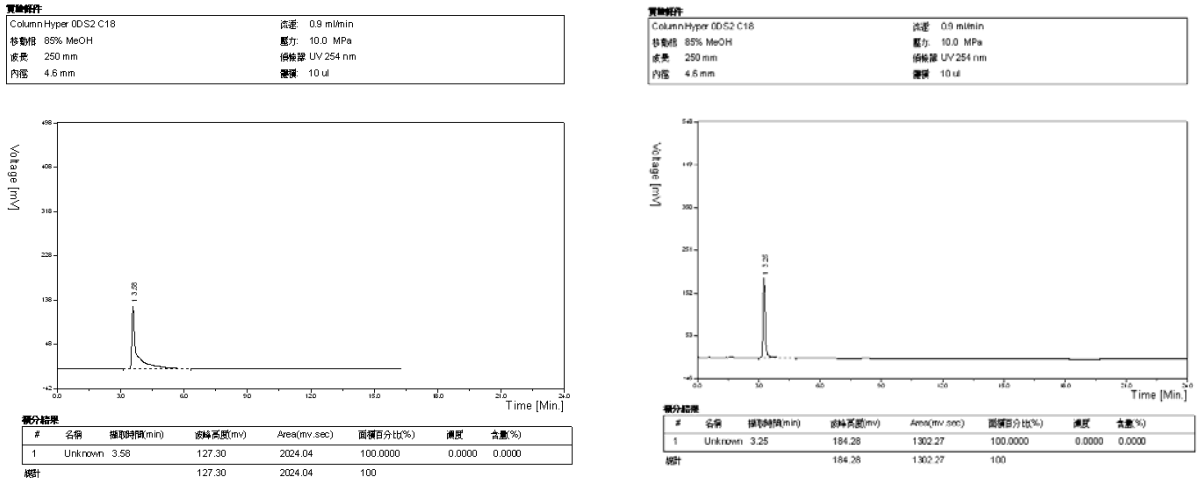

Fig. S12 Chromatograms of HPLC analysis of a) 4BPy-*m*DTC, b) 3BPy-*m*DTC, c) 2BPy-*m*DTC and d) BP-*m*DTC.

References

1) Y.-H. Chen, H.-H. Chou, T.-H. Su, P.-Y. Chou, F.-I. Wu and C.-H. Cheng, *Chem. Commun.* 2011, **47**, 8865.

2) J.-J. Lin, W.-S. Liao, H.-J. Huang, F.-I. Wu and C.-H. Cheng, *Adv. Funct. Mater.* 2008, **18**, 485.